# Shear Flow and Large Strain Oscillation of Dense Polymeric Micelle Suspension

**Taco Nicolai* and Lazhar Benyahia**

*Polymères, Colloïdes, Interfaces, UMR CNRS, Université du Maine, 72085 Le Mans Cedex 9, France*

*Received July 1, 2005; Revised Manuscript Received September 9, 2005*

ABSTRACT: Poly(ethylene oxide) (PEO) hydrophobically end-capped with an octadecyl group forms spherical micelles in water that resemble multiarm star polymers. The micelles jam (gel) at high concentrations after cooling below a critical temperature showing a discontinuous liquid−solid transition. The rheology of jammed micelle suspensions was studied utilizing both shear flow and oscillation. The flow rate was found to decrease with decreasing stress following a power law down to at least $10^{-5}$ $s^{-1}$, and neither a yield stress nor a flow rate independent viscosity was observed. Shear flow induces a first normal stress difference that is proportional to the shear stress and relaxes exponentially after cessation of flow. When the shear stress approaches a critical value, the flow rate increases more sharply and becomes independent of the shear stress at the critical value. The response to oscillatory shear is linear only for deformations less than 1%. The nonlinear response to large strain oscillation can be viewed as a superposition of the linear viscoelastic response and the strongly shear stress dependent flow. At a given shear stress the flow rate increases with increasing temperature.

## Introduction

Polymers containing a relatively small insoluble end group form spherical micelles above the critical micellar concentration.[1−3] These polymeric micelles resemble star polymers with the essential difference that the number of arms is not fixed. In dense suspensions, they often show a distinct liquid−solid transition when varying the temperature or the concentration, which is correlated with the appearance of a liquid crystalline phase. However, the formation of a crystalline phase is not necessary for the formation of the solid. When increasing the volume fraction of spherical particles[4−6] or multiarmed star polymers,[7−9] the viscosity diverges as the particles jam in an amorphous glassy state. A liquid−solid transition induced by a change in temperature has also been observed for amorphous star polymer suspensions.[9] The transition occurred without significant change of the structure factor of the system.

When a large enough shear stress is applied, jammed particle suspensions will flow.[4−7] Shear flow influences the crystalline structure of jammed polymeric micelles in order to allow for the flow.[10] Flow at low shear rates may induce increased alignment of the structure, while high shear rates can lead to complete breakup of the long-range order.

Water-soluble polymeric micelles are generally based on poly(ethylene oxide) (PEO). Micelles formed by di- or triblock copolymers of PEO with poly(propylene oxide) (PPO) (Pluronic) or poly(butylene oxide) (PBO) have been studied extensively.[1,2] A complication for these systems is that the hydrophobicity of PPO and PBO varies with the temperature, causing a temperature-dependent critical micellar concentration. In this sense, PEO polymers end-capped with short alkyl chains may be simpler. PEO end-capped at both ends, often via a urethane group (HEUR), have been investigated extensively for their thickening properties at relatively low concentrations.[11−16] The increase of the viscosity at low concentrations is caused by bridging of the micelles. At high concentrations these polymers form a body-centered-cubic (bcc) phase.[15] Large PEO chains end-capped at one end with short alkyl chains have been little investigated.[17]

Recently, a detailed study was reported of the liquid−solid transition of polymeric micelles based on PEO with molar mass 5000 kg/mol end-capped at one end with an octadecyl group.[18] In dilute solution these polymers form micelles with in aggregation number of 26 that is independent of the temperature and concentration below 100 g/L but increases at high concentrations. Above a concentration of about 150 g/L the solutions show a liquid−solid transition when cooling. It was shown that the transition is discontinuous, i.e., either the viscosity is less than about 0.2 Pa·s or the system does not flow for weeks when tilted. Solutions with intermediate viscosities are not stable and more or less rapidly transform to either of the two states. The upper limit of the viscosity for stable suspensions was independent of the polymer concentration, but the temperature where the transition occurred increased with increasing concentration.

A sharp liquid−solid transition over a very narrow temperature range is found also for other polymeric micelles,[19,20] but it has not been investigated for these systems whether the transition is discontinuous. Small-angle X-ray scattering (SAXS) showed that a body-centered-cubic phase is formed in the solid. However, when the dense PEO micelle suspensions are cooled rapidly, they jam before the crystalline order appears.[18] The structure with liquid order is unchanged through the liquid−solid transition, and the crystalline order appears after more than 10 min and stabilizes within an hour. The amount of crystalline order is very small close to the transition but increases with decreasing temperature and increasing concentration.

Here, an investigation is presented of the rheology of dense suspensions of these PEO micelles in the jammed state using both continuous shear flow and oscillation. Polymeric micelles have been studied extensively, but systematic investigations of the flow properties and the effect of large-amplitude oscillation are relatively rare. The existence of a yield stress is often assumed but is

10.1021/ma0514267 CCC: $30.25 © 2005 American Chemical Society
Published on Web 10/14/2005

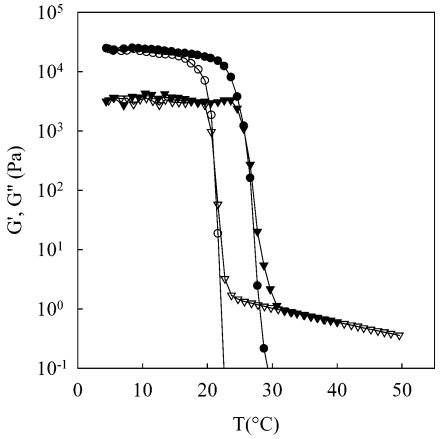


**Figure 1.** Temperature dependence of the storage (circles) and the loss (triangles) modulus during cooling (open) and heating (closed) at 1 Hz of a suspension of PEO micelles with $C = 200$ g/L. The cooling rate was 5 °C/min, and the stress was 5 Pa.

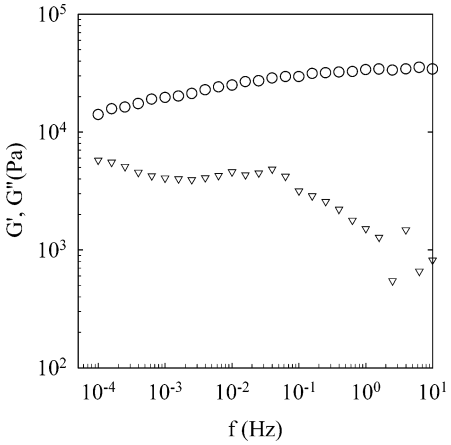


**Figure 2.** Frequency dependence of the storage (circles) and the loss (triangles) modulus of a suspension of PEO micelles with $C = 200$ g/L in the linear regime. The temperature was 20 °C, and the stress was 25 Pa.

not unambiguously established.[20−25] It will be shown that for the system studied here the flow rate in the jammed state decreases with decreasing stress following a power law down to at least $10^{-5}$ s$^{-1}$ without any sign of a yield stress. We also observed the development of a shear stress dependent normal stress difference that develops during shear flow, which, as far as we know, has not been reported before. Finally, we made a systematic study of the effect of shear stress and frequency during large-amplitude oscillation. The results will be interpreted in terms of the sum of an essentially elastic response and the stress-dependent flow term obtained from the flow experiments.

## Experimental Section

**Materials.** PEO end-capped with octadecyl was purchased from Aldrich (Brij700). The weight-average molar mass, $M_w = 4.0$ kg/mol (about 90 ethylene oxide segments), and polydispersity index, $M_w/M_n = 1.05$, were determined using size exclusion chromatography and static light scattering. Clear solutions were obtained in "Millipore" water after heating at 80 °C and agitating for about 15 min. The concentrations were obtained by weight and are expressed in g/L, since the density of the solutions is very close to 1 kg/L over the whole concentration range.

**Methods.** Dynamic mechanical measurements were done on a stress-controlled rheometer (AR1000, TA Instruments) using a cone−plate geometry (diameter 4 cm; angle 0.58°). In one experiment a plate−plate geometry was used (diameter 4 cm; gap 1 mm). The temperature was controlled using a Peltier system. Solvent evaporation was avoided by covering the geometry with mineral oil.

## Results

The rheometer was loaded with a solution containing 200 g/L of polymers in the liquid state. The temperature was reduced at a rate of 5 °C/min, during which the storage ($G'$) and the loss modulus ($G''$) were measured at 1 Hz using a stress of 5 Pa (see Figure 1). The liquid−solid transition is clearly observed by the strong increase of both $G'$ and $G''$. The transition can be reversed by heating, but the melting temperature is higher than the freezing temperature (see Figure 1). The difference between the freezing and the melting temperature decreases with decreasing cooling and heating rates.

The frequency dependence of the jammed systems was measured at 25 Pa, which is in the linear regime. At temperatures below the transition, $G' > G''$ over a very broad frequency range (see Figure 2). $G'$ has a very weak frequency dependence, whereas $G''$ decreases with increasing frequency. However, the experimental error is high at the low shear stresses where the response is linear. The frequency dependence of $G'$ and $G''$ is similar to those reported for other polymeric micelles.[26−28] In the jammed state $G'$ varies little with the temperature and increases weakly with increasing concentration.[18]

**Continuous Flow.** Creep experiments were done over a range of stresses. A linear increase of the strain as a function of time is observed after a transitional period that increases with decreasing stress. The shear rate ($\dot\gamma$) was calculated from the slope in the stationary regime. In Figure 3a $\sigma$ is plotted as a function of $\dot\gamma$ in a double-logarithmic representation for $C = 200$ g/L at 10 °C and shows a power law dependence down to at least $\dot\gamma = 10^{-5}$ s$^{-1}$: $\sigma \propto \dot\gamma^{0.17}$. At lower stresses we still observe creep, but it takes longer than 24 h to obtain a constant flow rate. It follows that the dynamic viscosity decreases with $\dot\gamma$ as $\eta \propto \dot\gamma^{-0.83}$ (see Figure 3b). There is no indication either for a divergence of $\eta$ characteristic for a solid with a yield stress or for a leveling off characteristic for a shear thinning liquid.

For $\sigma > 700$ Pa a steeper increase of $\dot\gamma$ is found until above a critical value of 855 Pa the flow rate diverges. Just above the critical shear stress the shear rate is initially almost constant, but then it accelerates and $\dot\gamma$ diverges. The delayed increase of $\dot\gamma$ is only observed just above the critical stress; at higher stresses the divergence of $\dot\gamma$ is immediate. An example of the delayed divergence is shown in Figure 4. The results shown in Figures 3 and 4 were obtained by measuring the shear rate at a fixed stress. Only in this way can very low shear rates be probed. In separate experiments the shear stress was measured at fixed high shear rates. It was found that steady shear flow at higher shear rates up to at least 100 s$^{-1}$ occurred at a constant shear stress close to the critical value. Values of the critical shear stress between 500 and 1000 Pa were observed at different concentrations and temperatures.

However, for a given concentration and temperature the critical stress is not well-defined because the systems are weakly modified by the flow. For a given stress the shear rate sometimes decreases very slowly with time (see for an example Figure 5). We observed this effect to varying extent for all samples. Apparently,

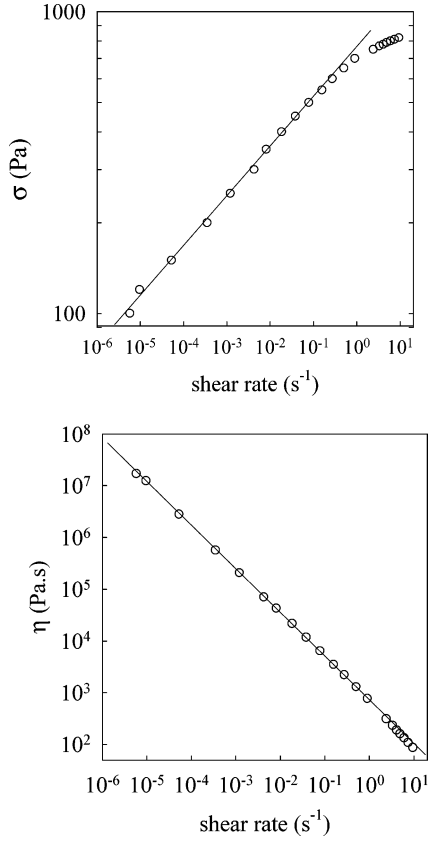


**Figure 3.** Double-logarithmic representation of the dependence of the shear rate on the shear stress (a) and of the dynamic viscosity on the shear rate (b) for a suspension of PEO micelles with $C = 200$ g/L at 10 °C. The solid lines have slopes 0.17 and −0.83, respectively.

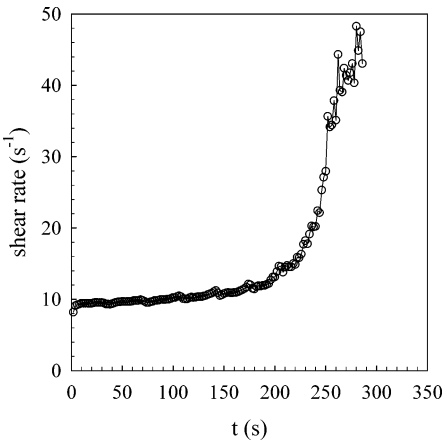


**Figure 4.** Example of the evolution of the shear rate for a dense suspension of PEO micelles close to the critical stress ($C = 200$ g/L, $\sigma = 820$ Pa, $T = 5$ °C).

the systems reinforce somewhat under flow. The effect is stronger at higher shear rates below the critical shear stress but is not reproducible in detail. However, flow at very high shear rates where it is independent of the stress leads to a weakening of the systems so that subsequent measurements at lower stresses give higher shear rates. If the same sample is reheated and cooled again, the shear rate will be slightly different at the same shear stress. Clearly, the absolute values of $\dot{\gamma}$ at a given shear stress depends somewhat on the sample history. Nevertheless, the power law dependence of $\dot{\gamma}$ on $\sigma$ is the same for a given temperature, and only the prefactor varies somewhat. We note that the effect of

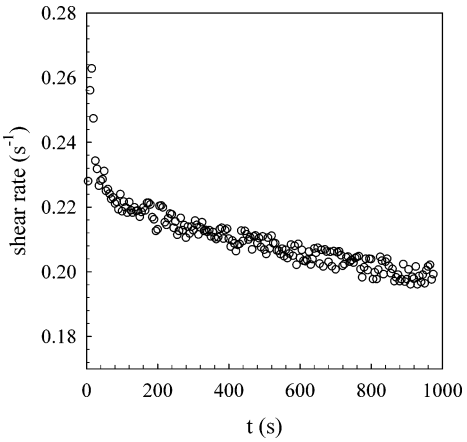


**Figure 5.** Example of the effect of flow hardening for a dense suspension of PEO micelles ($C = 200$ g/L, $\sigma = 500$ Pa, $T = 5$ °C).

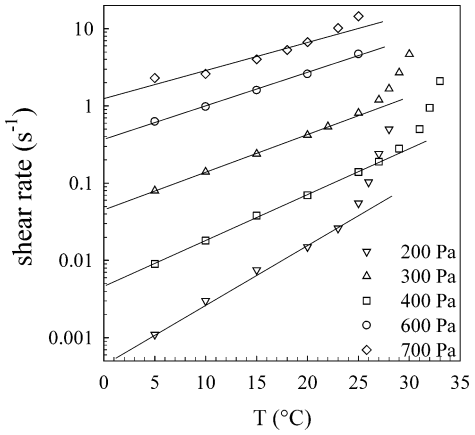


**Figure 6.** Temperature dependence of the shear rate at different shear stress indicated in the figure for a dense suspension of PEO micelles with $C = 200$ g/L.

shear history is only observed in flow experiments. The storage and loss modulus observed with oscillation in the linear regime was not influenced by the shear history as was reported also for other systems.[25,29,30]

Figure 6 shows the temperature dependence of $\dot{\gamma}$ at different stresses. Far below the melting temperature $\dot{\gamma}$ increases exponentially with increasing temperature, suggesting an activated process. The temperature dependence becomes weaker with increasing shear stress and is small close to the critical stress, which means that the critical stress is not very sensitive to the temperature. When the temperature approaches the melting temperature, a stronger increase of $\dot{\gamma}$ is observed until it diverges at a critical temperature in much the same manner as observed when increasing the stress at a constant temperature. The critical temperature where the shear rate diverges in the flow experiments is close to the melting temperature observed during oscillation with small deformations. When the temperature is increased at fixed shear rate, the shear stress decreases weakly followed by a strong decrease at the same melting temperature independent of the shear rate. The exponent α of the power law dependence on $\sigma$ ($\dot{\gamma} \propto \sigma^{\alpha}$) increases with decreasing temperature; e.g., we found for $C = 200$ g/L $\alpha = 6$ at 10 °C and $\alpha = 5$ at 20 °C.

As soon as the jammed systems start to flow, a normal force appears that increases with time until it reaches a plateau. No normal force was observed for the liquid

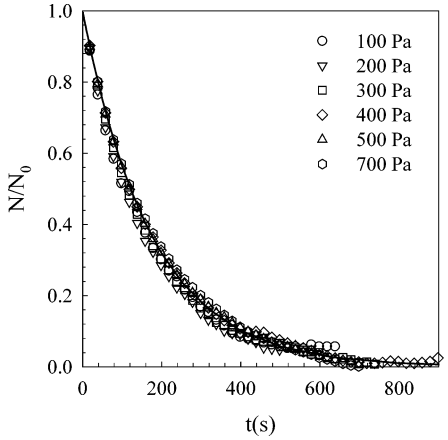


**Figure 7.** Relaxation of the normalized first normal stress difference after cessation of flow at different stresses indicated in the figure for a dense suspension of PEO micelles with $C$ = 300 g/L at 35 °C. The solid line represents a single-exponential decay with relaxation time 180 s.

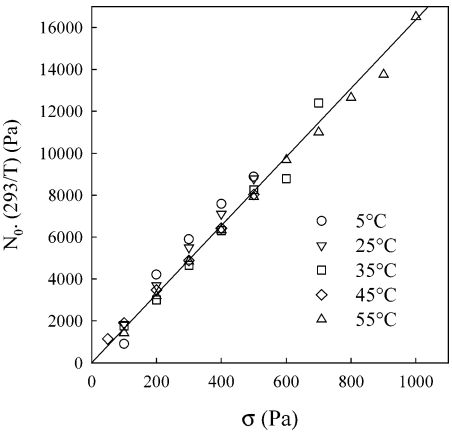


**Figure 8.** Dependence of the amplitude of the first normal stress difference as a function of the stress at different temperatures indicated in the figure for a dense suspension of PEO micelles with $C$ = 300 g/L. The slope of the solid line is 16.

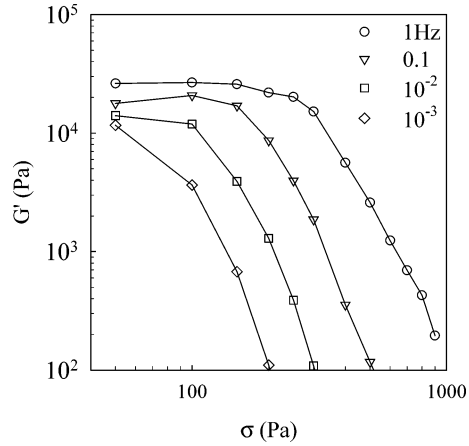


**Figure 9.** Dependence of the storage modulus on the stress at different frequencies indicated in the figure during shear oscillation of a dense suspension of PEO micelles with $C$ = 200 g/L at 20 °C.

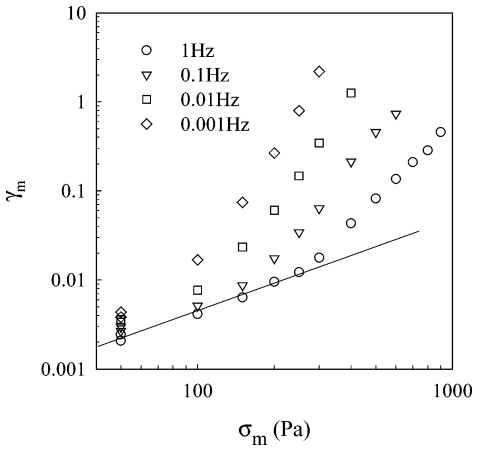


**Figure 10.** Dependence of the maximum deformation on the maximum stress at different frequencies during shear oscillation of a dense suspension of PEO micelles with $C$ = 200 g/L at 20 °C. The solid line has slope unity. The symbols are as in Figure 9.

samples. After cessation of the stress the normal force relaxes back. We note that about 1% strain is recovered after the stress is stopped. The strain is recovered rapidly and represents the maximum elastic deformation of the micelles. The relaxation of the first normal stress difference ($N$) is much slower and shows a single-exponential decay characterized by the same relaxation time at all shear stresses (see Figure 7). The amplitude ($N_0$) normalized by the absolute temperature ($T$) increases linearly with $\sigma$ (see Figure 8): $N_0(293/T) = 16\sigma$. The behavior was found to be the same at all temperatures tested for both 200 and 300 g/L. The relaxation of $N$ is a well-defined single exponential in all cases with an almost constant relaxation time of 180 s. However, the rise of $N$ is described by the same exponential as the relaxation only for low stresses. At higher shear stresses the increase of $N$ is limited to a maximum value of about 5000 Pa. In these cases the relaxation after cessation of the flow results in a negative normal force, which relaxes back to zero over time scales that are an order of magnitude slower. The amplitude of the normal force shown in Figure 8 is defined as the amount that relaxes following a single exponential. The results shown here are obtained using cone and plate geometry, but similar observations were made using plate−plate geometry.

**Oscillation.** In oscillation a sinusoidal variation of the shear stress is imposed, and the resulting deformation is determined starting after halve a cycle in the stationary regime. The shear stress may thus be written as $\sigma(t) = \sigma_m \cos(\omega t)$, where $\omega$ is the radial frequency related to the oscillation frequency as $\omega = 2\pi f$. In the linear response regime the deformation is related to stress through the storage ($G'$) and the loss modulus ($G''$) as follows: $\gamma(t) = \sigma_m(G' \cos(\omega t) + G'' \sin(\omega t))/(G'^2 + G''^2)$,[31] and an ellipsoid is observed if $\gamma(t)$ is plotted as a function of $\sigma(t)$ in a so-called Lissajous plot. If deviations from this shape occur, only apparent values of $G'$ and $G''$ are calculated, with no clear physical meaning.

The frequency dependence of the storage and the loss modulus was determined at different values of $\sigma_m$ for a solution containing 200 g/L PEO at 20 °C. We observed an apparent relaxation of the shear modulus that shifts to higher frequencies with increasing maximum. Figure 9 shows that the linear response regime where $G'$ and $G''$ are independent of $\sigma_m$ reduces to lower stresses with decreasing frequency. In Figure 10 the strain amplitude ($\gamma_m$) is plotted as a function of $\sigma_m$ at different frequencies. At low stresses $\gamma_m$ increases linearly with $\sigma_m$: $\gamma_m = \sigma_m/G'$, where $G'$ ($\gg G''$) is the value obtained in the linear regime. However, above a characteristic value

($\sigma^*$), $\gamma_m$ increases more rapidly. With decreasing frequency the increase of $\gamma_m$ is sharper and starts at lower $\sigma^*$. Figure 10 shows that the maximum strain amplitude where the response is linear is about 1% and decreases weakly with decreasing frequency because $G'$ decreases weakly.

$\gamma(t)$ is plotted in the left panel of Figure 11 for different values of $\sigma_m$ at a fixed frequency of 0.01 Hz. The corresponding Lissajous plots are shown in the right panel of Figure 11. An increasing deviation from the sinusoidal and elliptic shapes was found when increasing $\sigma_m$ beyond the linear regime. At $f = 0.01$ Hz we found $\gamma_m = 7 \times 10^{-5}\sigma_m$ in the linear regime, and the nonlinearity is negligible for $\sigma_m < 100$ Pa, i.e., $\gamma_m < 0.7\%$. The response becomes almost steplike at large stresses. Similar behavior has been reported for micelle suspensions formed by styrene−butadiene[21] and PBO−PEO[32] block copolymers.

At fixed $\sigma_m$ the nonlinearity increases with decreasing frequency (see Figure 12). In fact, very similar strain response is obtained at different frequencies if $\sigma_m$ is chosen such that $\gamma_m$ is the same. The close correspondence shows that increasing $\sigma_m$ is equivalent to decreasing $f$.

## Discussion

Dense suspensions of PEO micelles form an elastic solid for deformations less than 1%. It is clear that the elasticity of the system is not caused by the formation of a liquid crystalline order. With decreasing temperature the shear modulus increases sharply before any crystalline order is observed.[18] In addition, the amount of crystalline order increases strongly with decreasing temperature, while $G'$ has only a very weak temperature dependence. One may speculate that the origin of the elasticity is entropic due to deformation of the PEO chains that form the close packed micelles. In that case the shear modulus is proportional to the concentration of PEO chains: $G_e = RTC/M$, with $R$ the gas constant, which is compatible with the observed concentration and the temperature dependence of $G'$. Using $M = 4.0$ kg/mol, one obtains $G_e = 1.2 \times 10^5$ Pa for $C = 200$ g/L at 20 °C, which is about 4 times larger than $G'$ at high frequencies, indicating that not all chains are independently deformed. The shear modulus is independent of time and is not influenced significantly by the shear history. Watanabe et al.[29] suggested that the lower shear modulus is caused by correlation of the deformation of several chains in the micelle, which therefore act as a single elastic chain. The increase of $G''$ and the decrease of $G'$ with decreasing frequency in the linear regime indicates that some spontaneous relaxation of the stress is possible perhaps through hopping or restructuring of the micelles.[33,34]

The linear response domain during oscillatory shear is limited to very small strains. Apparently the micelles can only be deformed by about 1% before they start flowing. At higher deformations the systems flows and whatever the total deformation only an elastic part of about 1% is recovered. Similar maximum elastic strain amplitudes were reported for dense suspensions of micelles based on PPO−PEO[25,35] and PBO−PEO[30] block copolymers. For hard and soft spherical particles[5,6] somewhat higher maximum elastic deformations of 5−10% are reported.

A steady flow rate is obtained as soon as the deformation is significantly higher than the elastic deformation, i.e., about 1%. The flow rate decreases with decreasing stress following a steep power law, but neither a yield stress nor a flow rate independent viscosity is observed even for flow rates as low as $10^{-5}$ s$^{-1}$. It is generally considered that jammed micelle suspensions have a yield stress, based on the observation that the flow rate decreases dramatically below a certain stress. This is also the case for the systems studied here that do not flow over a period of weeks when tilted because at the shear stress induced by gravity the flow rate is simply to small. The idea of a yield stress, however, is that the system does not flow at all at lower stresses. It is debatable whether yield stresses defined in this sense exist.[36]

Jammed micelle suspensions have been rarely studied at very slow shear rates. They show a very weak increase of the stress with increasing shear rate at low rates followed by a stronger increase at higher rates.[24,25,29] Similar observations were made for sterically[5,6] or charge stabilized spheres[37] and emulsions.[38] The yield stress is estimated as the value below which the shear rate becomes very weakly dependent on the stress. However, the systems creep continuously at stresses below the yield stress determined in this way, and the value of the yield stress is not well-defined. Nevertheless, it was concluded that a distinction could be made between a flowing system above the yield stress and a creeping system below the yield stress.

Clearly, such a distinction cannot be made for the present system. The shear stress increases weakly at low shear rates following a power law dependence and subsequently becomes independent of the shear rate at higher values. Eiser et al.[25,39] also observed for micelles based on PPO−PEO diblock copolymers with a bcc structure that when they increased the flow rate, it became independent of the shear stress at values similar to those found for the present system. However, the same system with a face-centered-cubic (fcc) order showed a weak but continuous increase of the shear stress when increasing the shear rate for micelles. It was concluded that the system with the fcc structure had a yield stress and the system with the bcc order did not. They attributed the phenomenon observed for the system with the bcc structure to alignment of the crystalline domains. Such an alignment could also occur for the system studied here, but it would imply that the order is increased by shear because the degree of crystalline order in the absence of shear is low.[18]

To flow, the close-packed micelles need to slide over each other, which they can only do if they are slightly compressed. The flow rate decreases with decreasing temperature because excluded-volume interaction between PEO segments increases so that compression of the micelles takes more stress. Compression of the micelles might explain why the flow induces a normal force. The normal force is proportional to the shear stress, possibly because the number of compressed micelles is proportional to the shear stress. However, it takes a significant amount of time for the normal force to rise to its maximum value and to relax after cessation of flow, whereas the relaxation of the less than 1% elastic deformation is very rapid. This would suggest a structural change of the system under flow with a characteristic time scale of 180 s independent of the shear rate and also of the temperature and the concentration over the relatively small ranges investigated.

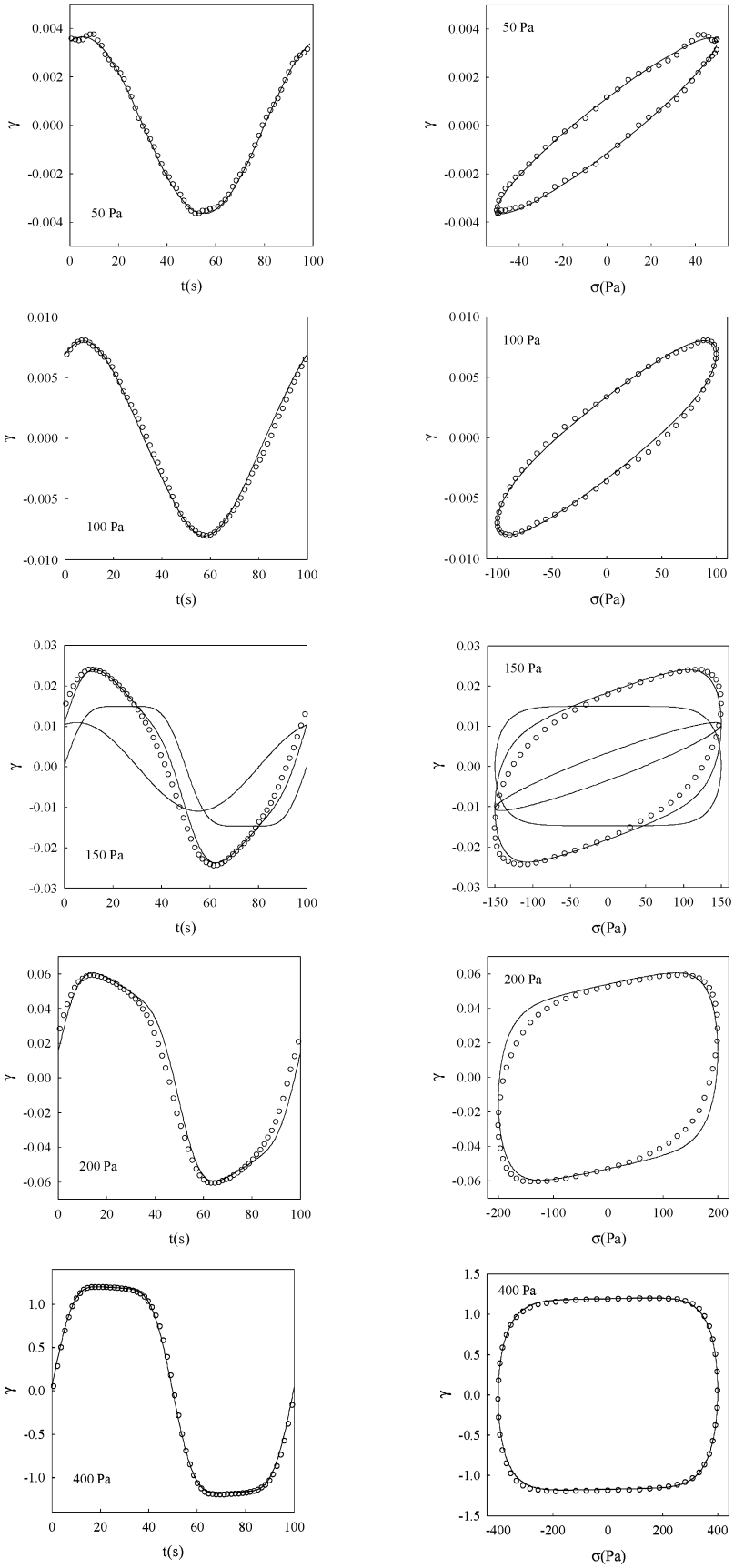


**Figure 11.** The left panel shows the strain response on oscillatory stress at 0.01 Hz and different maximum stresses indicated in the figure of a dense suspension of PEO micelles with $C = 200$ g/L at 20 °C. The corresponding Lissajous plots are shown in the left panel. The solid lines represent fits to eq 1.

Small-angle X-ray scattering measurements under shear will be needed to study structural modifications under flow. There are many studies showing that flow influences the structure of jammed micelles suspensions, and

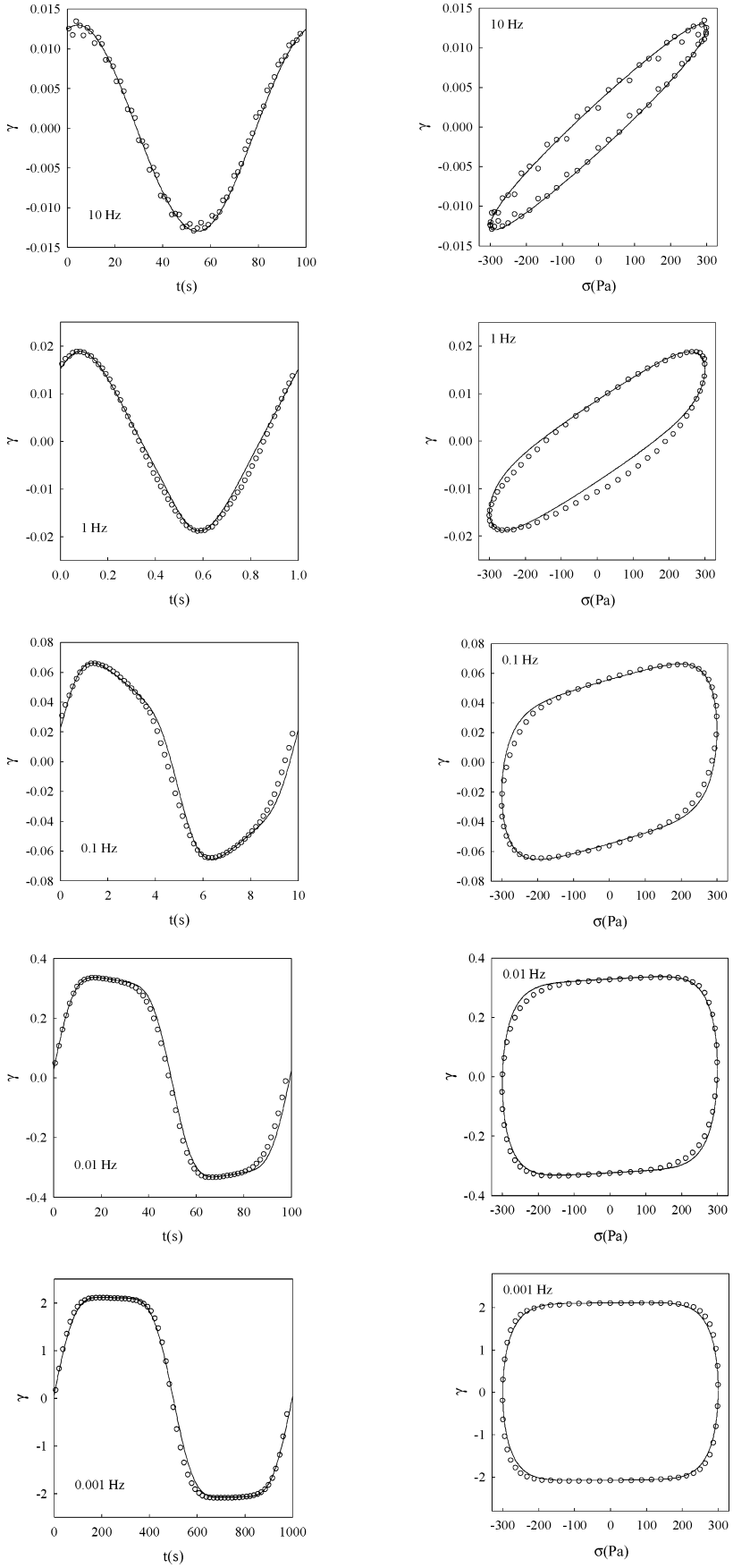


**Figure 12.** The left panel shows the strain response on oscillatory stress at $\sigma_m = 300$ Pa and at different frequencies indicated in the figure of a dense suspension of PEO micelles with $C = 200$ g/L at 20 °C. The corresponding Lissajous plots are shown in the left panel. The solid lines represent fits to eq 1.

one cannot exclude that structural modifications in turn influence the flow.[9] It is possible that the dependence of the flow rate on the shear history of the sample and the flow-induced reinforcement are caused by such a

structural modification.

Deviations from the power law dependence of the shear rate on the stress or the temperature were observed when the critical stress ($\sigma_c$) or melting temperature ($T_m$) is approached. Close to $\sigma_c$ and $T_m$ the shear rate has an even weaker dependence on the shear stress, indicating the transition to a different flow mechanism. For $T > T_m$ we observed a steady viscous flow with a viscosity that is independent of the shear stress and that decreases exponentially with increasing temperature. It was shown in ref 18 that $T_m$ increases with increasing concentration of the micelles and is correlated to the temperature dependence of their thermodynamic volume. On the other hand, for $\sigma > \sigma_c$ the flow rate diverges and flow rates higher than about 10 $s^{-1}$ occur at approximately the same shear stress. $\sigma_c$ does not depend strongly on the temperature and was about the same at 200 and 300 g/L, for which $T_m$ is 27 and 60 °C, respectively. $\sigma_c$ varies between 700 and 1000 Pa depending on the shear history of the samples.

The response to oscillationary stress becomes nonlinear if the maximum deformation exceeds about 1%. The Lissajous plots increasingly deviate from the ellipsoidal shape with decreasing frequency or increasing shear stress. Similar observations were made for suspensions of other polymeric micelles.[21,32] Even though deviation of the linear response is only clearly observed when $\gamma_m > 0.01$, irreversible particle displacements may have already occurred. Hebraud et al.[38] observed for a dense suspension of soft spheres that the fraction of irreversibly displaced particles increased continuously with increasing deformation even for deformations where macroscopically no sign of flow was observed.

The response to oscillation at higher deformations can to a large extent be understood as a superposition of the linear viscoelastic response and a stress-dependent flow:

$$\gamma(t) = \frac{\sigma_m[G' \cos(\omega t) + G'' \sin(\omega t)]}{G'^2 + G''^2} + \int_0^t \dot{\gamma}(\sigma)\, dt' \quad (1)$$

The solid lines in Figures 11 and 12 represent eq 1 with the values of $G'$ and $G''$ obtained in the linear regime shown in Figure 2. The separate contributions of the two terms are shown for one system in Figure 11 where they are approximately equal. We used the experimentally observed power law dependence of the flow rate on the shear stress for $C = 200$ g/L at 20 °C: $\dot{\gamma} \propto \sigma^5$ and $\sigma(t) = \sigma_m \cos(\omega t)$. It was necessary to vary the prefactor between $1.0 \times 10^{-14}$ and $2.3 \times 10^{-14}$ in order to obtain the correct values of $\gamma_m$. Flow measurements on the same system gave $\dot{\gamma} = 2.4 \times 10^5 \sigma^5$, but as mentioned above, the prefactor depends somewhat on the sample history. The maximum shear rate during oscillation at different frequencies is close to the steady shear rate during flow at $\sigma_m$. The implication is that the shear rate reacts rapidly to variation of the stress, which is a necessary condition for the use of eq 1.

As expected, at low stresses and high frequencies the viscoelastic response dominates. The relative importance of the flow term decreases with decreasing deformation and becomes negligible for $\gamma_m < 0.01$. At large stresses and low frequencies where $\gamma_m \gg 0.01$ the flow term dominates. At both these extremes the experimental response is very well described by eq 1. However, when the contributions of both terms are comparable, deviations are seen, indicating a mutual influence between the flow and the viscoelastic response. The transition between the mainly elastic response of $\gamma_m$ and the sharper increase caused by flow is shown in Figure 10 and occurs at a characteristic stress ($\sigma^*$) where the two terms in eq 1 are equal. The first term is proportional to $\sigma_m$ and varies little with the frequency because the shear modulus is only weakly frequency dependent. The second term is proportional to $\sigma_m^5/f$, and consequently $\sigma^* \propto f^{-4}$, which is what we observed in the experiment. A more direct way of observing the transition between the viscoelastic response and the shear flow is obtained by plotting the maximum shear rate $\dot{\gamma}_m$ during oscillation as a function of the shear stress at different frequencies. If we define $\sigma^*$ as the value $\sigma_m$ where the contributions of the two terms in eq 1 to the flow rate are equal, then $\dot{\gamma}_m = \omega\sigma^*/G'[\sigma_m/\sigma^* + (\sigma_m/\sigma^*)^5]$. The data obtained at different frequencies should therefore superimpose if the reduced shear rate, $\dot{\gamma}_m G'/2\omega\sigma^*$, is plotted as a function of $\sigma_m/\sigma^*$. Figure 13 shows that this is indeed observed, and the predicted dependence is found (see solid line).

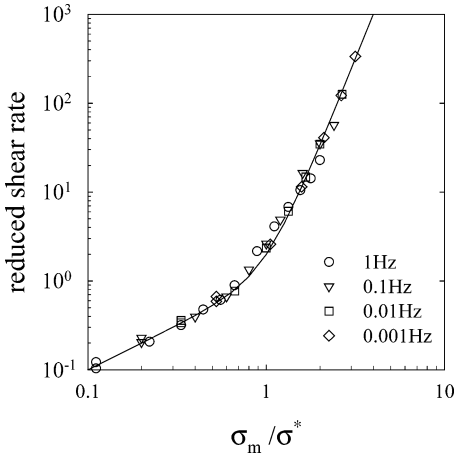


**Figure 13.** Dependence of the reduced maximum shear rate $\dot{\gamma}_m = \omega\sigma^*[G'/(G'^2 + G''^2)][\sigma_m/\sigma^* + (\sigma_m/\sigma^*)^5]$ as a function of the normalized maximum shear stress at different frequencies during shear oscillation of a dense suspension of PEO micelles with $C = 200$ g/L at 20 °C. The solid line represents $\sigma_m/\sigma^* + (\sigma_m/\sigma^*)^5$ unity.

The approach used here has some analogy to the model proposed by Doi et al.,[39] who supposed that the flow is caused by sliding layers when the stress exceeds a yield stress. At low deformations the system responds elastically while at high deformations the systems slips with a shear rate that increases linearly with the shear stress. As long as the deformation caused by flow is much smaller than the elastic deformation, one cannot distinguish between a true yield stress or very slow flow. Therefore, qualitatively the Lissajous plots obtained by this model look the same. However, the experimental results for the present system are different in detail because the flow rate has a much stronger than linear dependence on the shear stress.

Different behavior was observed in large strain oscillation of micelle suspension formed by PEO−PBO diblock copolymers. For this system different shapes of the Lissajous plots were observed at high strains that suggest strain hardening. In addition, the nonlinear response was not observed at lower frequencies.[32]

## Conclusions

Dense suspensions of polymeric micelles based on PEO jam below a critical temperature but still flow

when a shear stress is applied. The flow induces a normal force proportional to the shear stress probably caused by compression of the micelles. The flow rate decreases with decreasing stress following a power law, and no indication for a yield stress was found. At fixed shear stress the flow rate decreases with decreasing temperature because excluded-volume interaction between the micelles increases. At high flow rates the rate becomes independent of the shear stress.

During oscillationary shear in the linear regime the response is mostly elastic at least down to $10^{-4}$ Hz although some very slow relaxation of the stress was observed. The response at strains larger than about 1% can be largely understood by the addition of the strongly stress dependent flow on top of the linear viscoelastic response.

## References and Notes


(1) Hamley, I. W. *The Physics of Block Copolymers*; Oxford University Press: Oxford, 1998.
(2) Alexandris, P.; Lindman, B. *Amphipylic Block Copolymers*; Elsevier: Amsterdam, 2000.
(3) Bhatia, S. R.; Miurchid, A.; Joanicot, M. *Curr. Opin. Colloid Interface Sci.* **2001**, *6*, 471.
(4) Larson, R. G. In Larson, R. G., Ed.; *The Structure and Rheology of Complex Fluids*; Oxford University Press: New York, 1999; p 261.
(5) Petedekis, G.; Vlassopoulos, D.; Pusey, P. N. *J. Phys: Condens. Matter* **2004**, S3955.
(6) Jones, D. A. R.; Leary, B.; Boger, D. V. *J. Colloid Interface Sci.* **1991**, *150*, 84, 479.
(7) Roovers, J. *Macromolecules* **1994**, *27*, 5359.
(8) Vlassopoulos, D.; Fytas, G.; Pispas, S.; Hadjichristidis, N. *Physica B* **2001**, *296*, 184.
(9) Loppinet, B.; Stiakakis, E.; Vlassopoulos, D.; Fytas, G.; Roovers, J. *Macromolecules* **2001**, *34*, 8216.
(10) Hamley, I. W. *Curr. Opin. Colloid Interface Sci.* **2000**, *5*, 342.
(11) Lafleche, F.; Durand, D.; Nicolai, T. *Macromolecules* **2003**, *36*, 1331.
(12) Kaczmarski, J. P.; Glass, J. E. *Macromolecules* **1993**, *26*, 5149.
(13) Yekta, A.; Xu, B.; Duhamel, J.; Adiwidjaja, H.; Winnik, M. A. *Macromolecules* **1995**, *28*, 956.
(14) Annable, T.; Buscall, R.; Ettelai, R.; Whittlestone, D. *J. Rheol.* **1993**, *37*, 695.
(15) Alami, E.; Rawiso, M.; Isel, F.; Beinert, G.; Binane-Limbele, W.; François, J. *ACS Adv. Chem.* **1996**, *248*, 343.
(16) Alami, E.; Almgren; M.; Brown, W.; François, J. *Macromolecules* **1996**, *29*, 2230.
(17) Ameri, M.; Attwood, D.; Collett, J. H.; Booth, C. *J. Chem. Soc., Faraday Trans.* **1997**, *15*, 2545.
(18) Nicolai, T.; Lafleche, F.; Gibaud, A. *Macromolecules* **2004**, *37*, 8066.
(19) Brown, W.; Schillen, K.; Almgren, M.; Hvidt, S.; Bahadur, P. *J. Phys. Chem.* **1991**, *95*, 9788.
(20) Mingvanish, W.; Kelarakis, A.; Mai, S.-M.; Daniel, C.; Yang, Z.; Havredaki, V.; Hamley, I. W.; Ryan, A. J.; Booth, C. *J. Phys. Chem. B* **2000**, *104*, 9788.
(21) Watanabe, H.; Kotado, T.; Hashimoto, T.; Shibayama, M.; Kawai, H. *J. Rheol.* **1982**, *26*, 153.
(22) Hashimoto, T.; Shibayama, M.; Kawai, H.; Watanabe, H.; Kotado, T. *Macromolecules* **1983**, *16*, 361.
(23) Watanabe, H. *Acta Polym.* **1997**, *48*, 215.
(24) McConnel, G. A.; Lin, M. Y.; Gast, A. P. *Macromolecules* **1995**, *28*, 6754.
(25) Eiser, E.; Molino, F.; Porte, G.; Pithon, X. *Rheol. Acta* **2000**, *39*, 201.
(26) Buitenhuis, J.; Förster, S. *J. Chem. Phys.* **1997**, *107*, 262.
(27) Kelarakis, A.; Havredaki, V.; Derici, L.; Yu, G. E.; Booth, C.; Hamley, I. W.; Ryan, A. J. *J. Chem. Soc., Faraday Trans.* **1998**, *94*, 3639.
(28) Castelletto, V.; Hamley, I. A.; English, R. J.; Mingvanish, W. *Langmuir* **2003**, *19*, 3229.
(29) Watanabe, H.; Kanaya, T.; Takahashi, Y. *Macromolecules* **2001**, *34*, 662.
(30) Pople, J. A.; Hamley, I. A.; Fairclough, J. P. A.; Ryan, A. J.; Komanchek, B. U.; Gleeson, A. J.; Yu, G. E.; Booth, C. *Macromolecules* **1997**, *30*, 5721.
(31) Ferry, J. D. *Viscoelastic Properties of Polymers,* 3rd ed.; Wiley: New York, 1980.
(32) Hamley, I. A.; Pople, J. A.; Booth, C.; Derici, L.; Impéror-Clerc, M.; Davidson, P. *Phys. Rev. E* **1998**, *58*, 7620.
(33) Semenov, A. N.; Joanny, J.-F.; Khokhlov, A. R. *Macromolecules* **1995**, *28*, 1066.
(34) Sollich, P.; Lequeux, F.; Hébraud, P.; Cates, M. E. *Phys. Rev. Lett.* **1997**, *78*, 2020.
(35) Mortenson, K.; Brown, W.; Jorgenson, E. *Macromolecules* **1994**, *27*, 5654.
(36) Barnes, H. A. *J. Non-Newtonian Fluid Mech.* **1999**, *181,* 133.
(37) Fagan, M. E.; Zukoski, C. F. *J. Rheol.* **1997**, *41*, 373.
(38) Mason, T. G.; Bibette, J.; Weitz, D. A. *J. Colloid Interface Sci.* **1996**, *179*, 439.
(39) Eiser, E.; Molino, F.; Porte, G.; Diat, O. *Phys. Rev. E* **2000**, *61*, 6759.
(40) Hébraud, P.; Lequeux, F.; Munch, J. P.; Pine, D. J. *Phys. Rev. Lett.* **1997**, *78*, 4657.
(41) Doi, M.; Harden, J. L.; Ohta, T. *Macromolecules*, **1993**, *26*, 4935.


MA0514267